

Introduction:

➤ Task: Design a novel multi-category rotation detector for small, cluttered and rotated objects.

➤ Challenges:

- The inconsistency between metric and loss
- Boundary discontinuity
- Square-like problem

➤ Our main contributions:

- We summarize three flaws in state-of-the-art rotation detectors, i.e. inconsistency between metric and loss, boundary discontinuity, and square-like problem, due to their regression based angle prediction nature.
- We propose to model the rotating bounding box distance by Gaussian Wasserstein Distance (GWD) which leads to an approximate and differentiable IoU induced loss. It resolves the loss inconsistency by aligning model learning with accuracy metric and thus naturally improves the model.
- Our GWD-based loss can elegantly resolve boundary discontinuity and square-like problem, regardless how the rotating bounding box is defined. In contrast, the design of most peer works are coupled with the parameterization of box.

➤ Codes: <https://github.com/yangxue0827/RotationDetection>

Proposed Approach

➤ Most of the IoU-based loss can be considered as a distance function. Inspired by this, we propose a new regression loss based on Wasserstein distance. First, we convert a rotating bounding box $B(x,y,w,h,\theta)$ into a 2-D Gaussian distribution $N(m,\Sigma)$.

$$\Sigma^{1/2} = \mathbf{R}\mathbf{S}\mathbf{R}^T$$

$$= \begin{pmatrix} \cos\theta & -\sin\theta \\ \sin\theta & \cos\theta \end{pmatrix} \begin{pmatrix} \frac{w}{2} & 0 \\ 0 & \frac{h}{2} \end{pmatrix} \begin{pmatrix} \cos\theta & \sin\theta \\ -\sin\theta & \cos\theta \end{pmatrix}$$

$$= \begin{pmatrix} \frac{w}{2} \cos^2\theta + \frac{h}{2} \sin^2\theta & \frac{w-h}{2} \cos\theta \sin\theta \\ \frac{w-h}{2} \cos\theta \sin\theta & \frac{w}{2} \sin^2\theta + \frac{h}{2} \cos^2\theta \end{pmatrix}$$

$$\mathbf{m} = (x, y)^T$$

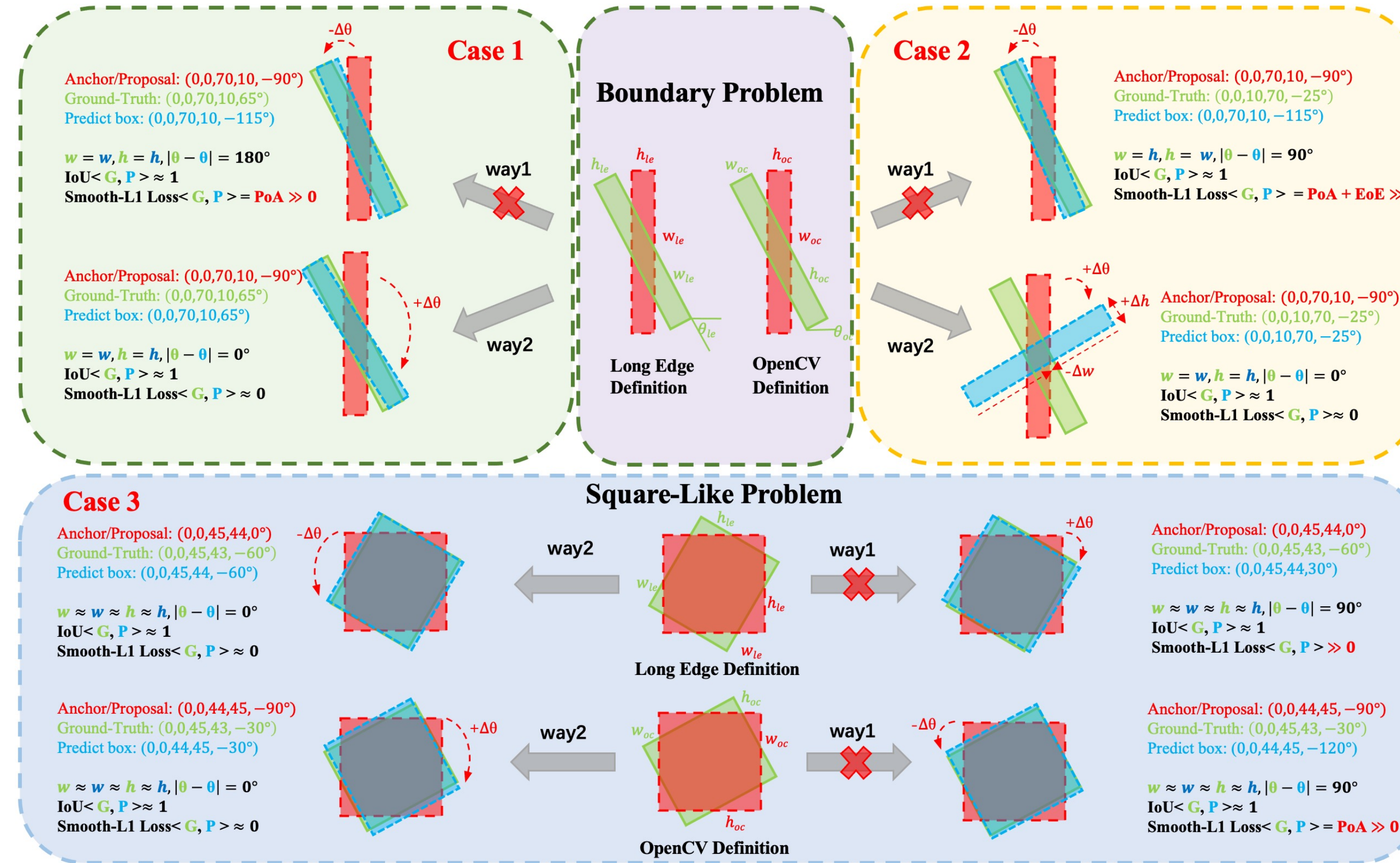
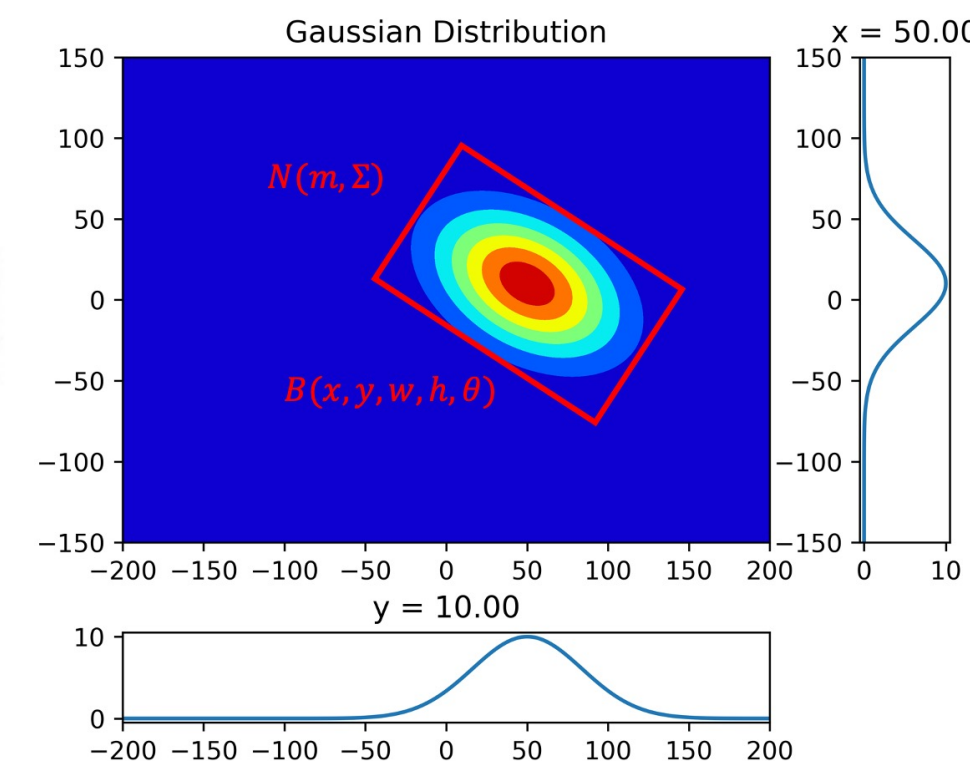


Figure 1. Boundary discontinuity under two bounding box definitions (top), and illustration of the square-like problem (bottom).

➤ GWD has the following properties to solve all the problems in Figure 1:

Property 1: $\Sigma^{1/2}(w, h, \theta) = \Sigma^{1/2}(h, w, \theta - \frac{\pi}{2})$;

Property 2: $\Sigma^{1/2}(w, h, \theta) = \Sigma^{1/2}(w, h, \theta - \pi)$;

Property 3: $\Sigma^{1/2}(w, h, \theta) \approx \Sigma^{1/2}(w, h, \theta - \frac{\pi}{2})$, if $w \approx h$.

➤ The Wasserstein distance between two probability measures can be expressed as follow:

$$d^2 = \|\mathbf{m}_1 - \mathbf{m}_2\|_2^2 + \text{Tr} \left(\Sigma_1 + \Sigma_2 - 2(\Sigma_1^{1/2} \Sigma_2 \Sigma_1^{1/2})^{1/2} \right)$$

➤ Gaussian Wasserstein Distance Regression Loss:

$$L = \frac{\lambda_1}{N} \sum_{n=1}^N obj_n \cdot L_{gwd}(b_n, gt_n) + \frac{\lambda_2}{N} \sum_{n=1}^N L_{cls}(p_n, t_n)$$

$$L_{gwd} = 1 - \frac{1}{\tau + f(d^2)}, \quad \tau \geq 1$$

Experiments:

➤ Ablation study for GWD on three dataset.

METHOD	BOX DEF.	REG. LOSS	DATASET	DATA AUG.	MAP ₅₀	
RETINANET	D_{oc}	SMOOTH L1	HRSC2016	R+F+G	84.28	
		GWD	HRSC2016		85.56 (+1.28)	
	D_{oc}	SMOOTH L1	UCAS-AOD		94.56	
		GWD	UCAS-AOD		95.44 (+0.88)	
	D_{oc}	SMOOTH L1	DOTA		F	65.73
		GWD				68.93 (+3.20)
D_{le}	SMOOTH L1	64.17				
	GWD	66.31 (+2.14)				
D_{oc}	SMOOTH L1	R ³ DET		70.66		
	GWD	R ³ DET		71.56 (+0.90)		

➤ Ablation study for GWD on two scene text datasets.

METHOD	REG. LOSS	DATASET	DATA AUG.	RECALL	PRECISION	HMEAN			
RETINANET	SMOOTH L1	MLT	F	37.88	67.07	48.42			
				GWD	44.01	71.83	54.58 (+6.16)		
	SMOOTH L1			R+F	71.55	68.10	69.78		
					GWD	73.95	74.64	74.29 (+4.51)	
	SMOOTH L1				ICDAR2015	R+F	69.43	81.15	74.83
							GWD	72.17	80.59
SMOOTH L1	R+F	69.09	80.30				74.28		
		GWD	70.00				82.15	75.59 (+1.31)	
SMOOTH L1		R+F	71.69	79.80			75.53		
			GWD	73.95			80.50	77.09 (+1.56)	

➤ Peer method comparison.

BASE DETECTOR	METHOD	BOX DEF.	IML	BD			TRAIN/VAL											
				EOE	POA	SLP	BR ¹	SV ¹	LV ¹	SH ¹	HA ¹	ST ¹	RA ¹	7-MAP ₅₀	MAP ₅₀	MAP ₇₅	MAP ₉₀	MAP ₉₅
RETINANET	IoU-SMOOTH L1 LOSS MODULATED LOSS	D_{oc}	✓	✓	✓	✓	42.17	65.93	51.11	72.61	53.24	78.38	62.00	60.78	65.73	64.70	32.31	34.50
							38.31	60.48	49.77	68.29	51.28	78.60	60.02	58.11	64.17	62.21	26.06	31.49
							42.92	67.92	52.91	72.67	53.64	80.22	58.21	61.21	66.05	63.50	33.32	34.61
							42.25	68.28	54.51	72.85	53.10	75.59	58.99	60.80	67.38	64.40	32.58	35.04
							41.40	65.82	56.27	73.80	54.30	79.02	60.25	61.55	67.39	65.93	35.66	36.71
							44.07	71.92	62.56	77.94	60.25	79.64	63.52	65.70	68.93	65.44	38.68	38.71
R ³ DET	DCL(BCL) GWD	D_{oc}	✓	✓	✓	✓	44.15	75.09	72.88	86.04	56.49	82.53	61.01	68.31	70.66	67.18	38.41	38.46
							46.84	74.87	74.96	85.70	57.72	84.06	63.77	69.70	71.21	67.45	35.44	37.54
							46.73	75.84	78.00	86.71	62.69	87.32	87.08	69.62	68.90	73.74	71.29	65.08

➤ AP on different objects and mAP on DOTA.

METHOD	BACKBONE	MS	PL	BD	BR	GTF	SV	LV	SH	TC	BC	ST	SBF	RA	HA	SP	HC	MAP ₅₀
ICN (AZIMI ET AL., 2018)	R-101	✓	81.40	74.30	47.70	70.30	64.80	67.80	70.00	90.80	79.10	78.20	53.60	62.90	67.00	64.20	50.20	68.20
ROI-TRANS. (DING ET AL., 2019)	R-101	✓	88.64	78.52	43.44	75.92	68.91	73.68	83.59	90.74	77.27	81.46	60.93	60.17	58.21	66.98	61.03	71.04
CAD-NET (ZHANG ET AL., 2019)	R-101	✓	87.8	82.4	49.4	73.5	71.1	63.5	76.7	90.9	79.2	73.3	48.4	60.9	62.0	67.0	62.2	69.9
SCRDET (YANG ET AL., 2019)	R-101	✓	89.98	80.65	52.09	68.36	68.36	60.32	72.41	90.85	87.94	86.86	65.02	66.68	66.25	68.24	65.21	72.61
FADET (LI ET AL., 2019)	R-101	✓	90.21	79.58	45.49	76.41	73.18	68.27	79.56	90.83	83.40	84.68	53.40	65.42	74.17	69.69	64.86	73.28
GLIDING VERTEX (XU ET AL., 2020)	R-101	✓	89.64	85.00	52.26	77.34	73.01	73.14	86.82	90.74	79.02	86.81	59.55	70.91	72.94	70.86	57.32	75.02
MASK OBB (WANG ET AL., 2019)	RX-101	✓	89.56	85.95	54.21	72.90	76.52	74.16	85.63	89.85	83.81	86.48	54.89	69.64	73.94	69.06	63.32	75.33
FEA (FU ET AL., 2020)	R-101	✓	90.1	82.7	54.2	75.2	71.0	79.9	83.5	90.7	83.9	84.6	61.2	68.0	70.7	76.0	63.7	75.7
APE (ZHU ET AL., 2020)	RX-101	✓	89.96	83.62	53.42	76.03	74.01	77.16	79.45	90.83	87.15	84.51	67.72	60.33	74.61	71.84	65.55	75.75
CENTERMAP (WANG ET AL., 2020A)	R-101	✓	89.83	84.41	54.60	70.25	77.66	78.32	87.19	90.66	84.89	85.27	56.46	69.23	74.13	71.56	66.06	76.03
CSL (YANG & YAN, 2020)	R-152	✓	90.25	85.53	54.64	75.31	74.44	73.51	77.62	90.84	86.15	86.69	69.60	68.04	73.83	71.10	68.93	76.17
RSDET-II (QIAN ET AL., 2021)	R-152	✓	89.93	84.45	53.77	74.35	71.52	78.31	78.12	91.14	87.35	86.93	65.64	65.17	75.35	79.74	63.31	76.34
SCRDET++ (YANG ET AL., 2020)	R-101	✓	90.05	84.39	55.44	73.99	77.54	71.11	86.05	90.67	87.32	87.08	69.62	68.90	73.74	71.29	65.08	76.81
PIGU (CHEN ET AL., 2020)	DLA-34	✓	80.9	69.7	24.1	60.2	38.3	64.4	64.8	90.9	77.2	70.4	46.5	37.1	57.1	61.9	64.0	60.5
O ² -DNET (WEI ET AL., 2020)	H-104	✓	89.31	82.14	47.33	61.21	71.32	74.03	78.62	90.76	82.23	81.36	60.93	60.17	58.21	66.98	61.03	71.04
P-RSDet (ZHOU ET AL., 2020)	R-101	✓	88.58	77.83	50.44	69.29	71.10	75.79	78.66	90.88	80.10	81.71	57.92	63.03	66.30	69.77	63.13	72.30
BBAVECTORS (YI ET AL., 2020)	R-101	✓	88.35	79.96	50.69	62.18	78.43	78.98	87.94	90.85	83.58	84.35	54.13	60.24	65.22	64.28	55.70	72.32
DRN (PAN ET AL., 2020)	H-104	✓	89.71	82.34	47.22	64.10	76.22	74.43	85.84	90.57	86.18	84.89	57.65	61.93	69.30	69.63	58.48	73.23
R ³ DET (YANG ET AL., 2021b)	R-152	✓	89.80	83.77	48.11	66.77	78.76	83.27	87.84	90.82	85.38	85.51	65.67	62.68	67.53	78.56	72.62	76.47
POLARDET (ZHAO ET AL., 2020)	R-101	✓	89.65	87.07	48.14	70.97	78.53	80.34	87.45	90.76	85.63	86.87	61.40	70.32	71.92	73.09	67.15	76.64
S ² A-NET-DAL (MING ET AL., 2020)	R-50	✓	89.69	83.11	55.03	71.00	78.30	81.90	88.46	90.89	84.97	87.46	64.41	65.65	76.86	72.09	64.35	76.95
R ³ DET-DCL (YANG ET AL., 2021a)	R-152	✓	89.26	83.60	53.54	72.76	79.04	82.56	87.31	90.67	86.99	86.98	67.49	66.88	73.29	70.69	69.99	77.37
RDD (ZHONG & AO, 2020)	R-101	✓	89.15	83.92	52.51	73.06	77.81	79.00	87.08	90.62	86.72	81.15	63.96	70.29	76.98	75.79	72.15	77.75
S ² A-NET (HAN ET AL., 2021)	R-101	✓	89.28	84.11	56.95	79.21	80.18	82.93	89.21	90.86	84.66	87.61	61.96	68.23	78.58	78.20	65.55	79.15
GWD (OURS)	R-152	✓	89.66	84.99	59.26	82.19	78.97	84.83	87.70	90.21	86.54	86.85	73.47	67.77	76.92	79.22	74.92	80.23